THE JOURNAL OF BIOLOGICAL CHEMISTRY VOL. 287, NO. 20, pp. 16689–16697, May 11, 2012

Hyaluronidase 1 and β-Hexosaminidase Have Redundant Functions in Hyaluronan and Chondroitin Sulfate Degradation*◆

Received for publication, February 7, 2012, and in revised form, March 13, 2012 Published, JBC Papers in Press, March 26, 2012, DOI 10.1074/jbc.M112.350447

Lara Gushulak[‡1], Richard Hemming[‡], Dianna Martin[§], Volkan Seyrantepe[¶], Alexey Pshezhetsky[‖], and Barbara Triggs-Raine[‡2]

From the [‡]Department of Biochemistry and Medical Genetics, University of Manitoba, Winnipeg, Manitoba R3E 0J9, Canada, the [§]Genetics and Genome Biology, The Hospital for Sick Children, Toronto, Ontario M5S 2Y9, Canada, the [¶]Department of Molecular Biology and Genetics, Faculty of Science, Izmir Institute of Technology, Gulbahce Koyu, Urla, 35430 Izmir, Turkey, and the [‖]Division of Medical Genetics, CHU Sainte-Justine, and the Department of Pediatrics, University of Montreal, 3175 Côte Sainte-Catherine, Montréal, Quebec H3T 1C5, Canada

Background: The individual contribution of HYAL1 and β-hexosaminidase to glycosaminoglycan (GAG) degradation is not fully understood.
Results: Mice deficient in both of these enzymes exhibit global accumulation of hyaluronan and related GAGs.
Conclusion: A functional redundancy exists between HYAL1 and β-hexosaminidase.
Significance: Investigating the contribution of individual hyaluronidases and exoglycosidases is critical to understanding the overall pathways of GAG catabolism.

Hyaluronan (HA), a member of the glycosaminoglycan (GAG) family, is a critical component of the extracellular matrix. A model for HA degradation that invokes the activity of both hyaluronidases and exoglycosidases has been advanced. However, no *in vivo* studies have been done to determine the extent to which these enzymes contribute to HA breakdown. Herein, we used mouse models to investigate the contributions of the endoglycosidase HYAL1 and the exoglycosidase β-hexosaminidase to the lysosomal degradation of HA. We employed histochemistry and fluorophore-assisted carbohydrate electrophoresis to determine the degree of HA accumulation in mice deficient in one or both enzyme activities. Global HA accumulation was present in mice deficient in both enzymes, with the highest levels found in the lymph node and liver. Chondroitin, a GAG similar in structure to HA, also broadly accumulated in mice deficient in both enzymes. Accumulation of chondroitin sulfate derivatives was detected in mice deficient in both enzymes, as well as in β-hexosaminidase-deficient mice, indicating that both enzymes play a significant role in chondroitin sulfate breakdown. Extensive accumulation of HA and chondroitin when both enzymes are lacking was not observed in mice deficient in only one of these enzymes, suggesting that HYAL1 and β-hexosaminidase are functionally redundant in HA and chondroitin breakdown. Furthermore, accumulation of sulfated chondroitin in tissues provides *in vivo* evidence that both HYAL1 and β-hexosaminidase cleave chondroitin sulfate, but it is a preferred substrate for β-hexosaminidase. These studies provide *in vivo* evidence to support and extend existing knowledge of GAG breakdown.

Hyaluronan (HA)[3] is a large polysaccharide made up of repeating units of GlcUA and GlcNAc. It is a member of the glycosaminoglycan (GAG) family that consists of several uronic-acid containing polymers that are defined by their unique repeating disaccharide units, including HA, chondroitin, and sulfated derivatives of chondroitin (1). HA is abundant in the extracellular matrix of vertebrate tissues, where it provides structural integrity to tissues and cells. In addition, HA has been shown to have functional roles in inflammation (2), ovulation (3), and other processes. Moreover, HA is used broadly in medical devices, medical treatments, and cosmetic applications (4). Despite the wide distribution of HA and its diverse roles in tissues, the pathways of its catabolism are still not completely understood.

A model for HA degradation was initially proposed by Hascall *et al.* (5) and further advanced by Stern (6, 7). This model proposes that the degradation begins with cleavage of high to low molecular weight HA by an extracellular hyaluronidase enzyme, HYAL2. HA fragments are then internalized through interactions with a cell surface receptor such as CD44 (8, 9), LYVE-1 (lymphatic vessel endothelial HA receptor-1) (10), or HARE (HA receptor for endocytosis) (11). Once internalized, the endosome matures to a lysosome, where other hyaluronidases break HA down to generate short oligosaccharides that

* This work was supported in part by Canadian Institutes of Health Research Grant MOP-89873.
◆ This article was selected as a Paper of the Week.
[1] Supported by a Canadian Institutes of Health Research studentship and a joint studentship from the Manitoba Health Research Council and the Manitoba Institute of Child Health.
[2] To whom correspondence should be addressed: Dept. of Biochemistry and Medical Genetics, University of Manitoba, 745 Bannatyne Ave., Winnipeg, Manitoba R3E 0J9, Canada. Tel.: 204-789-3218; Fax: 204-789-3900; E-mail: traine@cc.umanitoba.ca.

[3] The abbreviations used are: HA, hyaluronan; GAG, glycosaminoglycan; TKO, triple knock-out; DKO, double knock-out; HABP, HA-binding protein; FACE, fluorophore-assisted carbohydrate electrophoresis; 0S, chondroitin; 4S, chondroitin type A; 6S, chondroitin type C; UA2S, chondroitin 2-sulfate; S_E, chondroitin type E; S_B, dermatan sulfate.

are putative substrates for the lysosomal exoglycosidases β-glucuronidase and β-hexosaminidase (6). Recently, using C57BL/6 mice, it was shown that some HA degradation can occur locally, but most is degraded in the lymphatics, and low levels are also disposed of in the liver (12).

The lysosomal degradation of HA is supported by studies showing that inhibitors of lysosomal function disrupt HA degradation (9, 13). However, within the lysosome, the individual contributions of hyaluronidases and exoglycosidases to the breakdown of HA are still to be defined. Low molecular weight HA has been suggested as a potential substrate for the endoglycosidases HYAL1 and HYAL3 (6, 14). However, *HYAL1* is expressed highly in a broad range of tissues, whereas *HYAL3* is expressed at extremely low levels (15), suggesting that HYAL1 may play a larger role in the degradation of HA. Furthermore, human mutations in hyaluronidase-coding genes have been found only in *HYAL1* and cause mucopolysaccharidosis IX (OMIM 601492) (15, 16). Physical characteristics of mucopolysaccharidosis IX are limited primarily to cartilaginous tissues and are considered relatively mild compared with other mucopolysaccharidoses (15, 16).

Given the rapid turnover of HA in some tissues (4), substantial accumulation of HA was predicted in the absence of an enzyme required for its degradation. However, HA accumulation in multiple tissues was not identified in transgenic mice deficient in any one hyaluronidase (17–19). This lack of HA accumulation and the mild phenotype observed in HYAL1-deficient patients could potentially be explained by a functional redundancy between the highly expressed HYAL1 and another lysosomal HA-degrading enzyme.

One potential compensating enzyme, β-hexosaminidase (*N*-acetyl-β-D-glucosaminidase), is a lysosomal exoglycosidase that has been shown to cleave HA *in vitro* (1). The enzyme is coded for by *HEXA* and *HEXB*, which produce the α-subunit and β-subunit, respectively. Isoforms of the enzyme consist of an α-subunit homodimer (β-hexosaminidase S), a β-subunit homodimer (β-hexosaminidase B), and a heterodimer of both subunits (β-hexosaminidase A) (20). In humans, mutations of *HEXA* and *HEXB* are familiarly associated with the lysosomal storage disorders Tay-Sachs disease (OMIM 272800) and Sandhoff disease (OMIM 268800), respectively. These disorders, both categorized as GM2 gangliosidoses, are characterized by extensive accumulation of gangliosides that cannot be degraded in the absence of β-hexosaminidase A (21). Interestingly, however, mice deficient in all β-hexosaminidase isoforms ($Hexa^{-/-}$ $Hexb^{-/-}$) also demonstrate a mucopolysaccharidosis-like phenotype, which includes accumulation of both GAGs and gangliosides in multiple tissues (22, 23). The identity of these GAGs was not fully investigated and could therefore include HA and others. Monosaccharide analysis completed on urine excreted from mice deficient in all isoforms of β-hexosaminidase showed extensive accumulation of two monosaccharides common to the structure of dermatan sulfate (22). However, it has previously been shown that excretion of HA through the urinary system accounts for only 1% of normal HA turnover (24). Therefore, accumulation of HA in β-hexosaminidase-deficient mice may have been missed, as the identities of individual GAGs were not assayed in tissues.

In this study, we focused on the characterization of GAGs in a triple knock-out (TKO) mouse model deficient in HYAL1 and all isoforms of β-hexosaminidase. GAGs were also assayed in tissues from mice with deficiencies in either HYAL1 or β-hexosaminidase activity. These mouse models allowed us to explore the possibility of functional redundancies within the proposed model of HA breakdown. In addition, we were able to assess the contributions of these enzymes in the catabolism of other members of the GAG family. TKO mice displayed global HA accumulation, with the highest levels of HA in the liver and lymph node; this extensive accumulation of HA was not observed in mice deficient in only one of these enzyme activities. These results serve to further define the overall pathway of HA degradation, the major tissues involved, and the functional redundancies that exist in HA breakdown. Furthermore, the functional redundancy between β-hexosaminidase and HYAL1 may explain the mild phenotype observed in patients with a HYAL1 deficiency (15, 16, 25) and potentially create treatment options for these patients.

EXPERIMENTAL PROCEDURES

Generation of Experimental Animals—C57BL/6;C129 mice heterozygous for *Hexa* and *Hexb* gene disruptions ($Hexa^{+/-}$ $Hexb^{+/-}$) were characterized previously (26) and crossed with C57BL/6 mice heterozygous for a deletion in the *Hyal1* gene ($Hyal1^{+/-}$) that were purchased from MMRRC (MMRRC: 000086-UCD, Davis, CA) and have been described in detail (19). Mice heterozygous at all three loci ($Hexa^{+/-}$ $Hexb^{+/-}$ $Hyal1^{+/-}$) were bred to generate TKO mice ($Hexa^{-/-}$ $Hexb^{-/-}$ $Hyal1^{-/-}$), and double knock-out (DKO) sex-matched littermates ($Hexa^{-/-}$ $Hexb^{-/-}$ $Hyal1^{+/-}$) served as controls. Wild-type mice ($Hexa^{+/-}$ $Hexb^{+/+}$ $Hyal1^{+/+}$) were also generated from the above crosses. Mice with the correct genotypes were identified by PCR amplification of DNA from ear punches. The wild-type and disrupted *Hexa* and *Hexb* alleles were amplified as described previously (26), except the denaturing and annealing steps were programmed for 1 min. The wild-type *Hyal1* allele was amplified using established methods (19). However, because the disrupted alleles for *Hexa* and *Hexb* also contained a neomycin cassette, different primers and conditions were required to detect the deleted *Hyal1* allele. WPG 617 (5′-ATCGCCTTCTATCGCCTT-3′) and WPG 619 (5′-GAGACATGCCTTGAACTCTGCCTCC-3′) were used to amplify a 450-bp band using the same PCR conditions specified for the wild-type and disrupted *Hexa* and *Hexb* alleles (26).

TKO mice displayed severe neurological deterioration requiring euthanasia at ~4 weeks of age. Tissues from TKO mice, sex-matched DKO control littermates, and sex- and age-matched wild-type mice were collected, frozen at −80 °C for biochemical studies, or fixed in 10% buffered formalin (Fisher) containing 0.5% hexadecylpyridinium chloride (Sigma-Aldrich) for histological studies. Tissues fixed for histological studies were embedded in paraffin and sectioned at 5 μm. All procedures and care of the animals were in compliance with the Canadian Council on Animal Care and approved by the Animal Protocol Management and Review Committee at the University of Manitoba.

Histological Studies—H&E staining was completed to assess overall tissue morphology as described previously with some modifications (27). Mayer's hematoxylin was applied for 3 min, followed by a 6-min wash with running tap water and eosin incubation for 40 s. Alcian blue staining (pH 2.5) of GAGs in tissue sections was carried out as described (28), except the slides were counterstained with Nuclear Fast Red (ScyTek Laboratories) for 2.5 min. HA was localized in tissue sections by using the biotinylated HA-binding protein (HABP; Calbiochem) at 6.67 μg/ml as described (19), omitting the trypsin treatment step. Colorimetric development of positive staining was done with diaminobenzidine without nickel to produce a visible brown color. Slides were counterstained with hematoxylin for 2 min, followed by a 5-min wash with running tap water. Slides were then dehydrated, mounted, and visualized using bright-field microscopy.

Fluorophore-assisted Carbohydrate Electrophoresis—HA and other GAG levels in dried mouse tissues were quantified using fluorophore-assisted carbohydrate electrophoresis (FACE) as described previously (29) with the following adjustments. Following the deactivation of proteinase K (Sigma) by boiling, samples were extracted with acetone (3 parts acetone/1 part supernatant) and stored at −20 °C for 2 h. After the first ethanol precipitation, precipitates were pelleted, reconstituted with ultrapure water, and divided into three aliquots. Individual aliquots were treated with 5 milliunits of hyaluronidase SD (Seikagaku) or chondroitinase ABC (Sigma-Aldrich) in 200 mM ammonium acetate buffer using the pH recommended by the supplier. The third aliquot received no enzyme treatment and served as a negative control. Samples were incubated overnight at 37 °C. The resulting disaccharides were then isolated and labeled as described (29). Labeled disaccharide units were separated on a 20% acrylamide gel using previously described conditions (30). Fluorescence signals were imaged using a Fluor-S MultiImager (Bio-Rad) and quantified by comparison with fluorescently labeled disaccharide standards (Seikagaku) using Quantity One software. Unpaired Student's *t* tests were used to test for statistical significance, and p values <0.05 were considered significant.

RESULTS

Phenotype of Hexa$^{-/-}$ Hexb$^{-/-}$ Hyal1$^{-/-}$ (TKO) Mice—The phenotype of the TKO mice was found to be similar to that described previously for *Hexa$^{-/-}$ Hexb$^{-/-}$* (DKO) mice (22, 23) but more severe. A significant difference was observed between the life spans of the TKO and DKO mice ($p = 0.04$). At ~23 days, the TKO mice reached the predetermined humane end point of inability to feed and/or reduced mobility compared with an average of 33 days for the DKO mice. The TKO mice were smaller than their DKO littermates, and leading up to the humane end point, they displayed tremors, seizure-like episodes, and labored breathing. Both TKO mice and their DKO littermates displayed a broad nose typical of mucopolysaccaridoses in mouse models (17, 31, 32).

Tissue Morphology and Substrate Accumulation—Tissue sections from 4-week-old TKO and DKO mice stained with H&E showed pronounced cellular vacuolization compared with wild-type tissues (Fig. 1*A*). The cellular vacuolization was consistent with intracellular macromolecule accumulation. However, there was no apparent difference in the overall vacuolization of TKO tissues compared with DKO tissues. Vacuolization due to substrate accumulation was observed in multiple tissues and was typical of a lysosomal storage disorder.

Alcian blue staining of TKO and DKO tissue sections resulted in an intense specific blue staining in both TKO and DKO tissues, whereas wild-type tissues stained much weaker (Fig. 1*B*). Furthermore, the staining in some of the TKO tissues (liver, skin, and brain) was more intense that that in DKO tissues, indicating an increased level of GAG accumulation in these tissues. The greater accumulation of GAG in the TKO mice suggests a redundancy between HYAL1 and β-hexosaminidase.

Localization and Accumulation of HA in Tissues—The failure to detect GAG accumulation in HYAL1-deficient mice (19), together with demonstrated GAG accumulation in DKO mice (22), suggested that HA may be one of the accumulating GAGs in the DKO mice. Surprisingly, an elevation of HA was not detected in DKO tissues compared with wild-type tissues after employing histochemistry (Fig. 2). Therefore, we wanted to assess HA accumulation in tissues from mice lacking both HYAL1 and β-hexosaminidase activities. Fig. 2 shows the distribution of HA in the liver, skin, brain, and lung detected using HABP (brown straining). HA accumulation was apparent in the sinusoids of the liver (Fig. 2*A*), around the periphery of vacuolated neural cells in the brain (Fig. 2*G*), and in the mucosal folds of the bronchiole (Fig. 2*J*) in the TKO mice. DKO tissue controls (Fig. 2, *B*, *H*, and *K*) for the liver, brain, and lung lacked the distinct staining patterns observed in the TKO mice. In skin (Fig. 2, *D* and *E*), HA levels appeared to be similar in the TKO mice and DKO controls. Negative controls showing the remaining signal after digestion with hyaluronidase were completed on all tissues. Fig. 2 (*M*–*O*) shows representative negative controls for TKO, DKO, and wild-type lung tissue.

Identification and Quantification of GAGs by FACE—FACE was performed to identify and quantify the levels of various GAGs, including HA, in the tissues of TKO and DKO control mice. GAGs were isolated from tissues and digested to their unique disaccharide units for quantification. A representative gel is shown in Fig. 3.

Given that the liver and lymph node are major turnover tissues for displaced HA (33, 34), we wanted to quantify HA levels in these tissues from TKO mice using FACE (Fig. 4*A*). HA levels were found to have reached an average of 78 ng/mg in the liver, far higher than the average level of 0.8 ng/mg detected in DKO controls ($p = 0.003$, $n = 3$). Extensive accumulation was also seen in the lymph node, with levels reaching 48 ng/mg compared with 4 ng/mg in DKO controls ($p = 0.02$, $n = 3$). Interestingly, HA levels observed in TKO liver and lymph node were ~3.6- and 2.2-fold higher, respectively, than those in TKO skin, a tissue known to have a high concentration of HA. The GAG accumulation in the TKO mice was not limited to HA, as chondroitin, a GAG very similar in structure to HA, was found to be higher in the liver ($p = 0.001$, $n = 3$) and lymph node ($p = 0.0005$, $n = 3$) in TKO mice compared with DKO controls (Fig. 4*B*). In addition to HA and chondroitin accumulation, TKO liver samples displayed significant accumulation of some forms

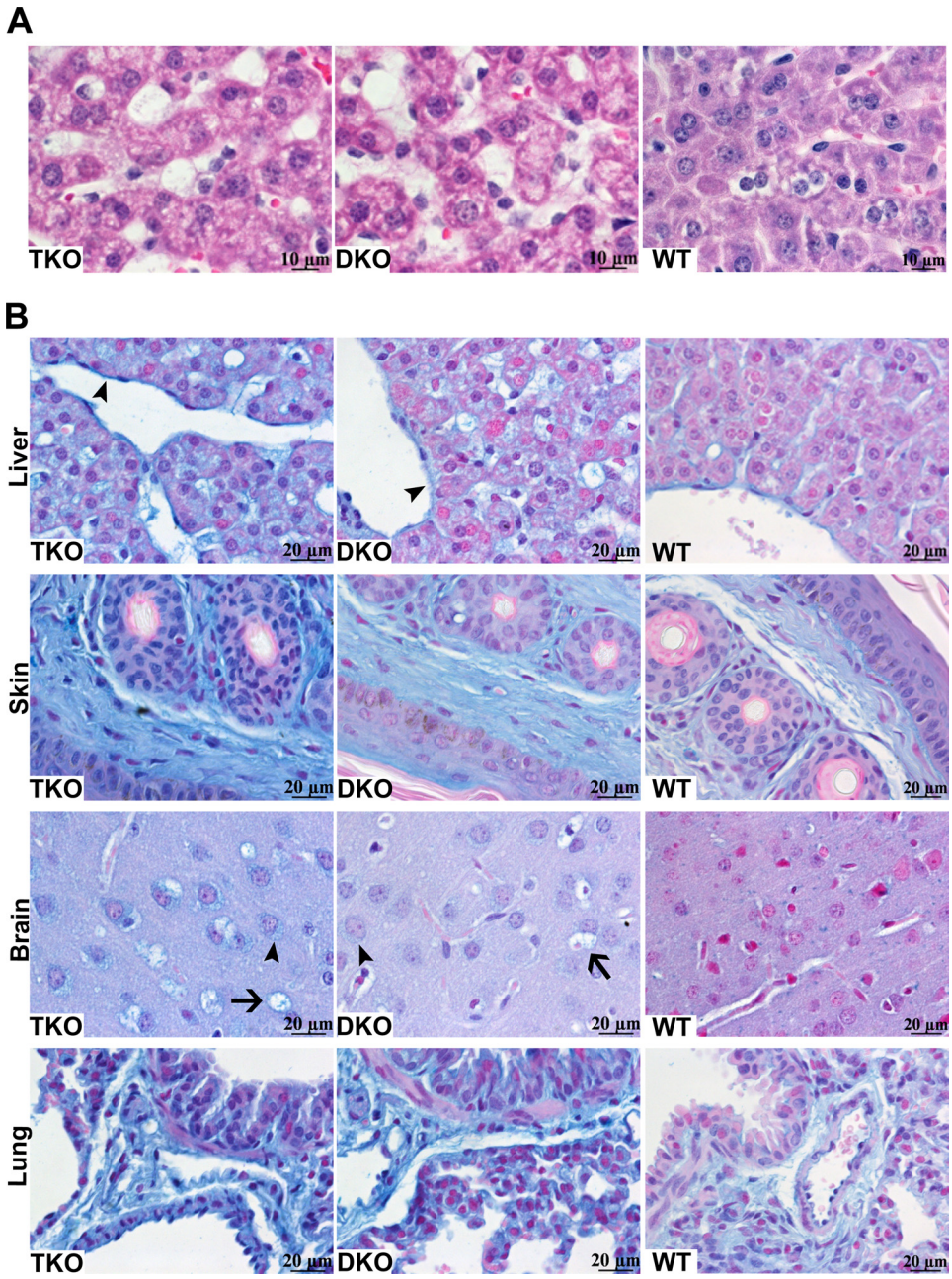

FIGURE 1. **Analysis of tissue morphology and GAG distribution in TKO, DKO, and wild-type mice.** *A*, H&E staining was completed to assess tissue morphology. The liver is shown as a representative tissue at ×100 magnification. Intracellular vacuolization was apparent in both TKO and DKO sections, but not in WT liver. *B*, tissue sections were stained with Alcian blue, and the presence of GAGs was observed (*blue* staining) at ×63 magnification. Compared with WT and DKO mice, TKO mice displayed more intense staining in the sinusoids of the liver (*arrowhead*), throughout the skin, and in the cytoplasm (*arrowhead*), as well as around vacuolated neural cells in the brain (*arrow*). Similar intensities of staining were seen in lung sections from TKO and DKO mice.

of sulfated chondroitin (Fig. 4*C*), including chondroitin 2-sulfate ($p = 0.005$, $n = 3$) and chondroitin type E ($p = 0.02$, $n = 3$).

Significant accumulation of HA in tissues that are not major areas of its overall turnover was also identified. In TKO brain ($p = 0.03$, $n = 3$) and lung ($p = 0.02$, $n = 4$), the concentration of HA was 5 and 3 ng/mg, respectively, whereas DKO controls displayed much lower levels in the brain (0.9 ng/mg) and lung (1 ng/mg) (Fig. 5*A*). Due to variation within the group, accumulation of HA in TKO skin ($p = 0.06$, $n = 5$) was not found to be statistically significant, although average levels (22 ng/mg) were ~4.4-fold higher than in DKO controls (5 ng/mg; $n = 4$). Similar to tissues with high levels of HA turnover, chondroitin also showed significant levels of accumulation in TKO skin, brain, and lung samples (Fig. 5*B*). Interestingly, brain samples from TKO mice displayed significant accumulation of sulfated chondroitin derivatives compared with DKO controls (Fig. 5*C*), although levels of sulfated chondroitin in TKO lymph node, skin, and lung were similar to DKO levels (data not shown).

Quantification of GAGs in Hyal1$^{-/-}$ and DKO Mice Using FACE—The identification of extensive HA accumulation in TKO tissues using FACE (Figs. 4*A* and 5*A*) was unexpected given the modest elevation in HA that was detected using the HABP (Fig. 2). Because previous studies of *Hyal1*$^{-/-}$-deficient mice focused on total GAG levels (19) and studies completed on

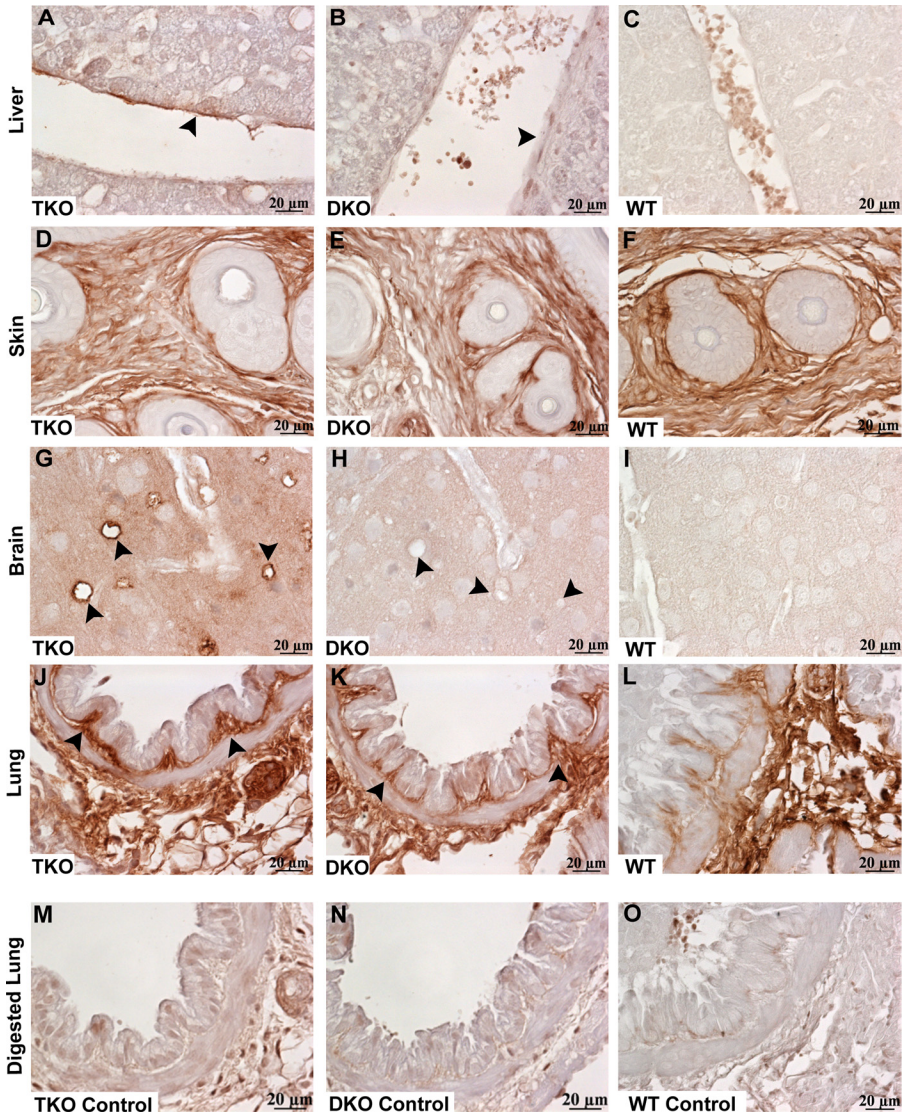

FIGURE 2. **HA localization in tissues of TKO, DKO, and WT mice.** HA was detected in tissue sections of TKO, DKO, and WT mice by staining with HABP, followed by viewing at ×63 magnification (*A–O*). Liver sections from TKO mice (*A*) displayed increased sinusoidal staining (*arrowhead*) compared with DKO controls (*B*) and WT liver (*C*). The skin (*D*, *E*, and *F*) was positive for HA, but the intensities were similar to each other. Brain sections from TKO mice (*G*) showed HA staining in the periphery of vacuolated neural cells (*arrowheads*), which was absent in DKO controls (*H*) and WT brain (*I*). HA accumulation was apparent in mucosal folds of the bronchiole (*arrowheads*) in TKO mice (*J*) compared with DKO controls (*K*) and WT lung (*L*). *M–O* served as negative controls, as the HA signal was not present after treatment with hyaluronidase from *Streptomyces hyalurolyticus*.

DKO mice used only monosaccharide analysis of urine (22) or HABP (Fig. 2), we decided to use FACE to examine GAG levels in tissues from mice with isolated deficiencies of either β-hexosaminidase or HYAL1. We used mice with a C57BL/6;C129 background, whereas previous *Hyal1*$^{-/-}$ studies were completed using C57BL/6 mice (19); therefore, where possible, FACE was performed on *Hyal1*$^{-/-}$-deficient tissues from both the C57BL/6 (previous studies) and C57BL/6;C129 (this study) backgrounds.

These studies allowed us to verify that the increase in HA seen in TKO tissues was a product of the loss of both HYAL1 and β-hexosaminidase activities. Of the β-hexosaminidase-deficient tissues examined, only the livers ($p = 0.04$, $n = 6$) and lymph nodes ($p = 0.02$, $n = 4$) of DKO mice demonstrated significant HA accumulation compared with the livers ($n = 5$) and lymph nodes ($n = 4$) of wild-type controls (Fig. 6*A*). These levels were ~41–608-fold lower than those seen in the livers and lymph nodes of TKO mice (Fig. 4*A*).

In the analysis of *Hyal1*$^{-/-}$ tissues from the C57BL/6;C129 background, no statistically significant elevation in HA was found compared with wild-type controls (Fig. 6*B*). However, a definite trend was apparent, with HYAL1-deficient tissues consistently showing higher levels of HA than observed in wild-type controls but lower levels than observed in the TKO tissues (Figs. 4 and 5). Significant HA accumulation was only seen in the livers ($p = 0.006$, $n = 4$) of C57BL/6 *Hyal1*$^{-/-}$ mice compared with wild-type controls (Fig. 6*C*), and again, these levels were ~660-fold lower than those observed in the TKO mice (Fig. 4*A*). Furthermore, this statistically significant elevation in HA was in tissues isolated from 1-year-old *Hyal1*$^{-/-}$ mice as part of a previous study (19). No tissues at early time points were available from the C57BL/6 line, and it is possi-

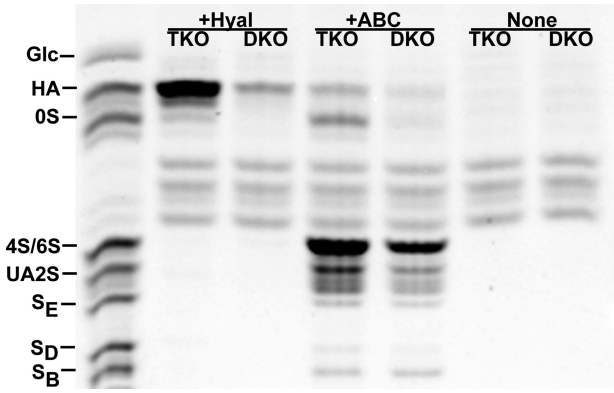

FIGURE 3. **FACE of various GAG disaccharides.** GAG disaccharides in TKO and DKO mouse tissue samples were analyzed using FACE. Tissue homogenates were digested with hyaluronidase SD (+*Hyal*) to produce HA disaccharides (GlcUA-GlcNAc). Chondroitinase ABC (+*ABC*) was used to generate disaccharides of chondroitin (0S; GlcUA-GalNAc) and its sulfated derivatives, including type A (4S; GlcUA-GalNAc4S), type C (6S; GlcUA-GalNAc6S), chondroitin 2-sulfate (UA2S; GlcUA-GalNAc2S), type E (S_E; GlcUA-GalNAc4,6S), type D (S_D; GlcUA2S-GalNAc6S), and dermatan sulfate (S_B; IdoA-GalNAc4S). A ladder of fluorescently labeled disaccharides was used to determine the position of each disaccharide. To serve as a negative control, an aliquot of the tissue homogenate was not digested (*None*).

ble that the observed accumulation in the liver would not be present at earlier time points. At the time of necropsy of the C57BL/6 *Hyal1*$^{-/-}$ mice, lymph nodes were isolated only for histological studies and were therefore not available for FACE studies.

Chondroitin did not accumulate in the DKO mice, C57BL/6; C129 *Hyal1*$^{-/-}$ mice, or C57BL/6 *Hyal1*$^{-/-}$ mice compared with wild-type controls (data not shown). Furthermore, in those tissues tested, no sulfated chondroitin derivatives were found to be accumulating in either background of *Hyal1*$^{-/-}$ mice compared with wild-type controls (data not shown). Interestingly, the DKO mice did show tissue-specific accumulation of various derivatives of chondroitin sulfate, with accumulation in the liver, lymph node, and lung (Fig. 7), but not in the brain or skin (data not shown).

DISCUSSION

The important structural and functional roles of HA make it a critical component of the extracellular matrix. Study of the degradation of this macromolecule within tissues has attracted interest from the extracellular matrix field for several years (5, 6, 12, 14). However, despite the development of several mouse models (17–19, 22, 23), the extent to which individual hyaluronidases and exoglycosidases participate in HA turnover was largely unknown. To gain further insight into the contribution of individual hyaluronidases and exoglycosidases in this process, we focused on two lysosomal enzymes proposed to be involved in the breakdown of HA using multiple mouse models. We have demonstrated that both the endoglycosidase HYAL1 and the exoglycosidase β-hexosaminidase are able to degrade HA fragments and other GAGs *in vivo*.

Ubiquitous accumulation of HA was found in mice genetically modified to have a combined deficiency of both HYAL1 and β-hexosaminidase activities. However, studies conducted in mice deficient in solely HYAL1 or β-hexosaminidase also showed tissue-specific accumulation of HA, albeit at much lower levels than seen with the combined deficiency. The HA accumulation observed after the loss of both HYAL1 and β-hexosaminidase activities can thus be attributed to a functional redundancy between the lysosomal hyaluronidase and the exoglycosidases β-hexosaminidase and β-glucuronidase. This redundancy may account for the relatively mild but still debilitating phenotype seen in human HYAL1-deficient patients (15, 16, 25), as β-hexosaminidase and β-glucuronidase would still be functional and able to degrade HA. Given the above redundancy, treatments that increase the amount of β-hexosaminidase and/or β-glucuronidase to supplement HA degradation in the joint could be useful in patients with HYAL1 deficiency.

Many studies have identified the lymph node and liver as principal sites of HA uptake and turnover (12, 24, 33–35); our results support these findings. Although TKO mice displayed global tissue accumulation of HA, the liver and lymph node showed much more extensive accumulation than the other tissues tested. A prior study of tissue HA distribution showed that the liver and lymph node normally have low levels of HA, whereas a tissue such as the skin has high levels of HA (24). Because the accumulated HA in the TKO liver and lymph node exceeded the concentration of that in tissues with high HA levels such as the skin, the HA is likely to have been transported to these tissues.

HA turnover studies suggest that peripheral tissue HA is brought to the lymph node, where it is degraded and recycled. Residual HA that reaches the blood is then sequestered by the liver and degraded (24, 36). TKO mice, deficient in both HYAL1 and β-hexosaminidase, displayed the highest level of HA accumulation in the liver, followed by the lymph node. However, mice deficient only in β-hexosaminidase displayed the greatest HA accumulation in the lymph node, with only a small accumulation in the liver. The former supports previous work suggesting that peripheral HA is first brought through the lymph to the lymph nodes, with a minor amount entering the bloodstream to the liver. Consequently, the organ distribution of HA accumulation in the TKO mice contradicts previous findings. However, based on the immense accumulation of HA globally in the TKO mice, the extensive amount of HA accumulated in the liver may just be a result of the liver having a greater overall HA storage capacity. Thus, with the lymphatic system at threshold, the efficiency of HA removal from the lymph would subsequently be hindered and allow more HA to be passed through the efferent lymphatics to the bloodstream and accumulate in the liver as a secondary site.

The broad HA accumulation observed in the TKO mice affected many tissues, including the brain. TKO mice displayed similar neurological deterioration as seen in the DKO controls, but the symptoms appeared ~10 days earlier. We suggest that the observed early deterioration is the result of neuronal toxicity due to the accumulation of multiple GAGs, including HA, as this accumulation was not seen in brain samples from mice deficient in either HYAL1 or β-hexosaminidase. The accumulation of other GAGs, primarily heparin sulfate, has previously been hypothesized as the cause of the neuropathy associated with several other mucopolysaccaridoses (38). Another possibility for the decreased life span is that the extensive accumu-

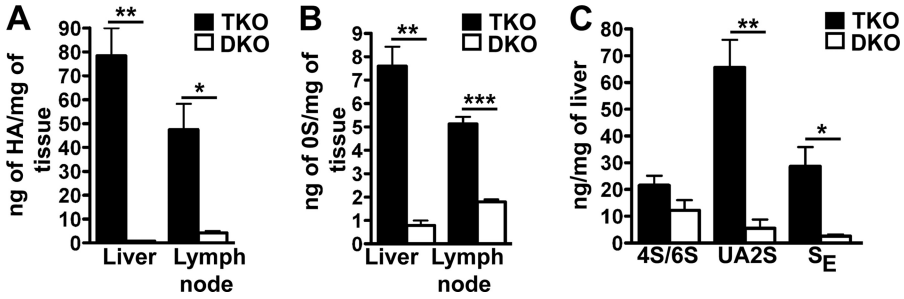

FIGURE 4. **Quantification of GAGs in high HA turnover tissues.** FACE was used to quantify HA (*A*), 0S (*B*), and sulfated chondroitin (*C*) in TKO and DKO liver ($n = 3$) and lymph node ($n = 3$). *A*, the level of HA was found to be significantly higher in TKO liver ($p = 0.003$) and lymph node ($p = 0.02$) compared with DKO controls. *B*, unlike DKO controls, TKO liver ($p = 0.001$) and lymph node ($p = 0.0005$) also significantly accumulated chondroitin. *C*, TKO liver samples also had significantly higher levels of UA2S ($p = 0.005$), and S_E ($p = 0.02$). 4S/6S ($p = 0.1$) did not significantly accumulate in TKO liver samples. Average levels of GAGs are shown in ng/mg of tissue with S.E. *, $p < 0.05$; **, $p < 0.01$; ***, $p < 0.001$.

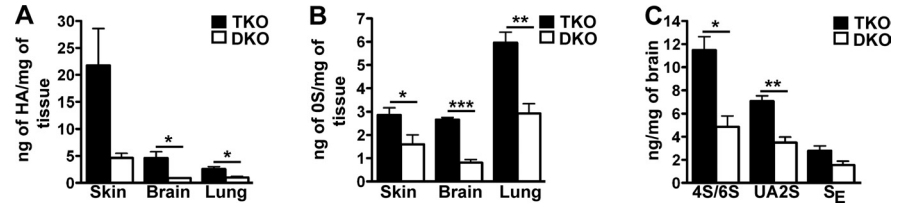

FIGURE 5. **Quantification of GAG accumulation in other tissues.** FACE was used to quantify HA (*A*), 0S (*B*), and sulfated chondroitin (*C*) in the skin, brain, and lung. *A*, HA levels were significantly higher in TKO brain ($p = 0.03$, $n = 3$) and lung ($p = 0.02$, $n = 4$) than in DKO controls. Accumulation of HA was not statistically significant in TKO skin samples ($p = 0.06$, $n = 5$). *B*, TKO skin ($p = 0.04$, $n = 5$), brain ($p = 0.0003$, $n = 3$), and lung ($p = 0.003$, $n = 4$) also had higher levels of chondroitin compared with DKO controls. *C*, TKO brain samples had significantly higher levels of 4S/6S ($p = 0.01$, $n = 3$) and UA2S ($p = 0.006$, $n = 4$). S_E levels did not differ significantly between the TKO and DKO samples ($p = 0.09$, $n = 4$). Average levels of GAGs are shown in ng/mg of tissue with S.E. *, $p < 0.05$; **, $p < 0.01$; ***, $p < 0.001$.

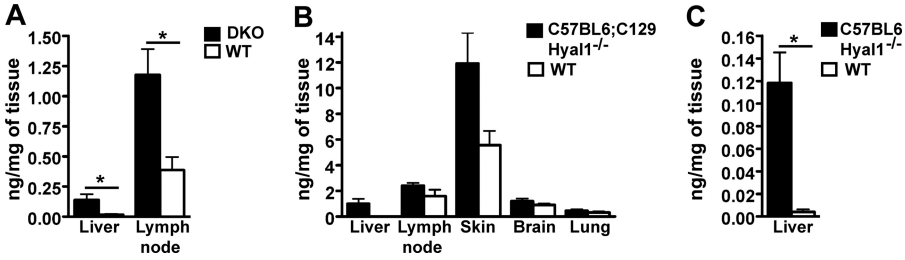

FIGURE 6. **Quantification of HA levels in DKO and *Hyal1*$^{-/-}$ mice compared with WT mice.** HA concentration was determined by FACE in mice deficient in either β-hexosaminidase (*A*) or HYAL1 (*B* and *C*). *A*, DKO mouse tissues with significant accumulation included the liver ($p = 0.04$, $n = 6$) and lymph node ($p = 0.02$, $n = 4$) compared with WT liver ($n = 5$) and lymph node ($n = 4$). *B*, C57BL/6;C129 *Hyal1*$^{-/-}$ mice ($n = 3$) did not significantly accumulate HA in any of the tissues tested; however, levels were consistently higher in HYAL1-deficient tissues than in WT tissues. *C*, C57BL/6 *Hyal1*$^{-/-}$ mice displayed accumulation in the liver ($p = 0.006$, $n = 4$). Average levels of GAGs are shown in ng/mg of tissue with S.E. *, $p < 0.05$.

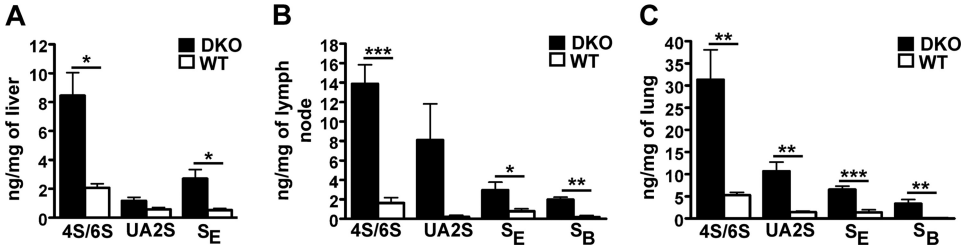

FIGURE 7. **Quantification of accumulating chondroitin sulfate derivatives in DKO mouse tissues.** Levels of chondroitin sulfate derivatives were quantified in DKO mice using FACE. Tissues with significant accumulation included the liver (*A*), lymph node (*B*), and lung (*C*). *A*, TKO liver ($n = 5$) significantly accumulated 4S/6S ($p = 0.01$) and S_E ($p = 0.02$) compared with WT liver ($n = 4$). UA2S levels were higher in DKO mice but not statistically significant ($p = 0.09$, $n = 5$). *B*, the lymph node accumulated significant levels of 4S/6S ($p = 0.0003$, $n = 5$), S_E ($p = 0.047$, $n = 4$), and S_B ($p = 0.001$, $n = 4$). UA2S levels in the DKO lymph node samples were higher than in WT samples; however, they were not statistically significant due to variation within the group ($p = 0.1$, $n = 3$). *C*, the lung accumulated significant levels of 4S/6S ($p = 0.005$, $n = 5$), UA2S ($p = 0.003$, $n = 5$), S_E ($p = 0.0006$, $n = 5$), and S_B ($p = 0.009$, $n = 5$). Average levels of GAGs are shown in ng/mg of tissue with S.E. *, $p < 0.05$; **, $p < 0.01$; ***, $p < 0.001$.

lation of GAGs reduced the efficacy of the lysosomal breakdown of other cellular material, resulting in cell toxicity. Regardless of the cause of early deterioration, the accumulation of HA after the loss of both HYAL1 and β-hexosaminidase indicates that HYAL1 plays an important role in HA degradation in the brain; this was surprising, as HYAL1 was previously thought to be weakly expressed in the brain (15). This finding suggests that the supplemental relationship between HYAL1 and β-hexosaminidase is critical for the proper breakdown of HA in the brain.

The presence of excess HA seems to be compatible with normal embryogenesis, as the TKO mice appeared normal at birth. This is in contrast to the hyaluronan synthase-2 knock-out mice, which die at embryonic day 9.5 due to a failure to synthesize HA (37). It seems likely that the presence of excess HA allows for normal development, and the failure to degrade HA does not lead to detectable symptoms until the postnatal period.

Along with HA accumulation, TKO mice also displayed global accumulation of non-sulfated chondroitin. This chondroitin is a GAG very similar to HA but is not a normal component of mouse tissues. This suggests that the chondroitin found in the TKO tissues may be derived from intermediates of chondroitin sulfate metabolism that have already been acted on by sulfatases. The presence of chondroitin in TKO (but not DKO or HYAL1-deficient) tissues provides evidence that a combined loss of HYAL1 and β-hexosaminidase activities affected the degradation pathways of multiple GAGs.

Previous studies have shown that like HA, sulfated chondroitin degradation occurs in the lysosome (39, 40) and that the same cell surface receptors for endocytosis are possibly shared (41, 42). Once within the lysosome, the contribution of each lysosomal enzyme to the degradation of sulfated chondroitin is unknown, but both a hyaluronidase (43) and an exoglycosidase (44) have been suggested to have a role. Recently, human HYAL4, thought to be a chondroitinase, was further characterized and confirmed to be a chondroitin sulfate-specific hydrolyase with little to no activity toward HA and dermatan sulfate (45). However, HYAL4 displays tissue-specific expression primarily in the placenta and skeletal muscle (46), suggesting that other enzymes also play a role in chondroitin sulfate degradation.

Sulfated derivatives of chondroitin were found to accumulate in a tissue-specific manner in mice lacking just β-hexosaminidase activity and in mice with the combined loss of HYAL1 and β-hexosaminidase. However, no accumulation was found in mice lacking only HYAL1 activity. β-Hexosaminidase-deficient mice accumulated several sulfated types of chondroitin, including that of dermatan sulfate, providing evidence that β-hexosaminidase has the ability to cleave multiple types of sulfated chondroitin *in vivo*. Furthermore, the accumulation of chondroitin sulfate in the brain and the additional accumulation in the liver after the combined loss of HYAL1 and β-hexosaminidase demonstrate, for the first time *in vivo*, that sulfated chondroitin derivatives are also substrates of HYAL1. Accumulation in the brain and liver implies that HYAL1 and β-hexosaminidase compensate for one another in a tissue-specific manner. The lack of chondroitin sulfate accumulation in other tissues such as the skin after the combined loss of HYAL1 and β-hexosaminidase implies that other enzymes are present, HYAL4 being a possible candidate.

In our study, a difference in the detection of HA when using HABP as opposed to FACE was apparent. Some possible explanations for this discrepancy include the effects of fixation and the specificity of HABP. Fixation of tissue can cause extraction of GAGs, resulting in a decreased signal. Frozen tissue was used for FACE analyses; and thus, extraction of GAGs was not a factor. It has also been shown that a decasaccharide is the smallest HA fragment able to strongly bind with the HABP (47, 48). Thus, it is possible that the accumulating HA in the paraffin tissue sections was not recognized because the size of intracellular HA may have been too small for detection. Therefore, we consider FACE as a more reliable assay for the detection and quantification of HA. Furthermore, the limitations of HABP need to be taken into account when this technique is used.

To conclude, this study describes extensive global accumulation of HA in mice that were modified to have a combined loss of HYAL1 and β-hexosaminidase activities. The lack of broad HA accumulation in mice deficient in either a hyaluronidase or an exoglycosidase suggests that there is a functional redundancy among the lysosomal HA-degrading enzymes, HYAL1, and β-hexosaminidase. Moreover, the loss of both HYAL1 and β-hexosaminidase activities creates an obstacle in overall GAG degradation as noted by the broad accumulation of chondroitin in the TKO mice, thus providing further evidence that HA and other GAGs share a common degradation route. Furthermore, for the first time *in vivo*, both HYAL1 and β-hexosaminidase were shown to degrade multiple types of chondroitin sulfate and to share a tissue-specific functional redundancy. Future studies combining the loss of other hyaluronidase-like enzymes will be required to determine whether and to what degree other hyaluronidases and exoglycosidases contribute to the degradation of HA and other GAGs.

Acknowledgments—We thank Xioali Wu and Steven Pind for technical guidance and advice.

REFERENCES

1. Meyer, K. (1969) Biochemistry and biology of mucopolysaccharides. *Am. J. Med.* **47,** 664–672
2. Jiang, D., Liang, J., and Noble, P. W. (2011) Hyaluronan as an immune regulator in human diseases. *Physiol. Rev.* **91,** 221–264
3. Russell, D. L., and Salustri, A. (2006) Extracellular matrix of the cumulus-oocyte complex. *Semin. Reprod. Med.* **24,** 217–227
4. Volpi, N., Schiller, J., Stern, R., and Soltés, L. (2009) Role, metabolism, chemical modifications, and applications of hyaluronan. *Curr. Med. Chem.* **16,** 1718–1745
5. Hascall, V. C., Sandy, J. D., and Handley, C. J. (1999) *Regulation of Proteoglycan Metabolism in Articular Cartilage: Biology of the Synovial Joint,* Harwood Academic Publishers, Amsterdam, The Netherlands
6. Stern, R. (2003) Devising a pathway for hyaluronan catabolism: are we there yet? *Glycobiology* **13,** 105R–115R
7. Stern, R. (2004) Hyaluronan catabolism: a new metabolic pathway. *Eur. J. Cell Biol.* **83,** 317–325
8. Harada, H., and Takahashi, M. (2007) CD44-dependent intracellular and extracellular catabolism of hyaluronic acid by hyaluronidases 1 and 2. *J. Biol. Chem.* **282,** 5597–5607
9. Culty, M., Nguyen, H. A., and Underhill, C. B. (1992) The hyaluronan receptor (CD44) participates in the uptake and degradation of hyaluronan. *J. Cell Biol.* **116,** 1055–1062
10. Banerji, S., Ni, J., Wang, S. X., Clasper, S., Su, J., Tammi, R., Jones, M., and Jackson, D. G. (1999) LYVE-1, a new homolog of the CD44 glycoprotein, is a lymph-specific receptor for hyaluronan. *J. Cell Biol.* **144,** 789–801
11. Zhou, B., Weigel, J. A., Fauss, L., and Weigel, P. H. (2000) Identification of the hyaluronan receptor for endocytosis (HARE). *J. Biol. Chem.* **275,** 37733–37741
12. Jadin, L., Bookbinder, L. H., and Frost, G. I. (2012) A comprehensive model of hyaluronan turnover in the mouse. *Matrix Biol.* **31,** 81–89
13. Rome, L. H., and Hill, D. F. (1986) Lysosomal degradation of glycoproteins and glycosaminoglycans. Efflux and recycling of sulfate and *N*-acetylhexo-

samines. *Biochem. J.* **235,** 707–713
14. Csoka, A. B., Frost, G. I., and Stern, R. (2001) The six hyaluronidase-like genes in the human and mouse genomes. *Matrix Biol.* **20,** 499–508
15. Triggs-Raine, B., Salo, T. J., Zhang, H., Wicklow, B. A., and Natowicz, M. R. (1999) Mutations in *HYAL1*, a member of a tandemly distributed multigene family encoding disparate hyaluronidase activities, cause a newly described lysosomal disorder, mucopolysaccharidosis IX. *Proc. Natl. Acad. Sci. U.S.A.* **96,** 6296–6300
16. Imundo, L., Leduc, C. A., Guha, S., Brown, M., Perino, G., Gushulak, L., Triggs-Raine, B., and Chung, W. K. (2011) A complete deficiency of hyaluronoglucosaminidase 1 (*HYAL1*) presenting as familial juvenile idiopathic arthritis. *J. Inherit. Metab. Dis.* **34,** 1013–1022
17. Jadin, L., Wu, X., Ding, H., Frost, G. I., Onclinx, C., Triggs-Raine, B., and Flamion, B. (2008) Skeletal and hematological anomalies in HYAL2-deficient mice: a second type of mucopolysaccharidosis IX? *FASEB J.* **22,** 4316–4326
18. Atmuri, V., Martin, D. C., Hemming, R., Gutsol, A., Byers, S., Sahebjam, S., Thliveris, J. A., Mort, J. S., Carmona, E., Anderson, J. E., Dakshinamurti, S., and Triggs-Raine, B. (2008) Hyaluronidase 3 (*HYAL3*) knock-out mice do not display evidence of hyaluronan accumulation. *Matrix Biol.* **27,** 653–660
19. Martin, D. C., Atmuri, V., Hemming, R. J., Farley, J., Mort, J. S., Byers, S., Hombach-Klonisch, S., Csoka, A. B., Stern, R., and Triggs-Raine, B. L. (2008) A mouse model of human mucopolysaccharidosis IX exhibits osteoarthritis. *Hum. Mol. Genet.* **17,** 1904–1915
20. Proia, R. L., d'Azzo, A., and Neufeld, E. F. (1984) Association of α- and β-subunits during the biosynthesis of β-hexosaminidase in cultured human fibroblasts. *J. Biol. Chem.* **259,** 3350–3354
21. Sandhoff, K., and Conzelmann, E. (1984) The biochemical basis of gangliosidoses. *Neuropediatrics* **15,** 85–92
22. Sango, K., McDonald, M. P., Crawley, J. N., Mack, M. L., Tifft, C. J., Skop E., Starr, C. M., Hoffmann, A., Sandhoff, K., Suzuki, K., and Proia, R. L. (1996) Mice lacking both subunits of lysosomal β-hexosaminidase display gangliosidosis and mucopolysaccharidosis. *Nat. Genet.* **14,** 348–352
23. Suzuki, K., Sango, K., Proia, R. L., and Langaman, C. (1997) Mice deficient in all forms of lysosomal β-hexosaminidase show mucopolysaccharidosis-like pathology. *J. Neuropathol. Exp. Neurol.* **56,** 693–703
24. Fraser, J. R., and Laurent, T. C. (1989) Turnover and metabolism of hyaluronan. *CIBA Found. Symp.* **143,** 41–53
25. Natowicz, M. R., Short, M. P., Wang, Y., Dickersin, G. R., Gebhardt, M. C., Rosenthal, D. I., Sims, K. B., and Rosenberg, A. E. (1996) Clinical and biochemical manifestations of hyaluronidase deficiency. *N. Engl. J. Med.* **335,** 1029–1033
26. Phaneuf, D., Wakamatsu, N., Huang, J. Q., Borowski, A., Peterson, A. C., Fortunato, S. R., Ritter, G., Igdoura, S. A., Morales, C. R., Benoit, G., Akerman, B. R., Leclerc, D., Hanai, N., Marth, J. D., Trasler, J. M., and Gravel, R. A. (1996) Dramatically different phenotypes in mouse models of human Tay-Sachs and Sandhoff diseases. *Hum. Mol. Genet.* **5,** 1–14
27. Allen, T. C. (1994) *Hematoxylin and Eosin: Laboratory Methods in Histotechnology,* American Registry of Pathology, Washington, D.C.
28. Gaffney, E. (1994) *Carbohydrates: Laboratory Methods in Histotechnology,* American Registry of Pathology, Washington, D.C.
29. Plaas, A. H., West, L., Midura, R. J., and Hascall, V. C. (2001) Disaccharide composition of hyaluronan and chondroitin/dermatan sulfate. Analysis with fluorophore-assisted carbohydrate electrophoresis. *Methods Mol. Biol.* **171,** 117–128
30. Lehrman, M. A., and Gao, N. (2003) Alternative and sources of reagents and supplies of fluorophore-assisted carbohydrate electrophoresis (FACE). *Glycobiology* **13,** 1G–3G
31. Vogler, C., Birkenmeier, E. H., Sly, W. S., Levy, B., Pegors, C., Kyle, J. W., and Beamer, W. G. (1990) A murine model of mucopolysaccharidosis VII. Gross and microscopic findings in β-glucuronidase-deficient mice. *Am. J. Pathol.* **136,** 207–217
32. Evers, M., Saftig, P., Schmidt, P., Hafner, A., McLoghlin, D. B., Schmahl, W., Hess, B., von Figura, K., and Peters, C. (1996) Targeted disruption of the arylsulfatase B gene results in mice resembling the phenotype of mucopolysaccharidosis VI. *Proc. Natl. Acad. Sci. U.S.A.* **93,** 8214–8219
33. Eriksson, S., Fraser, J. R., Laurent, T. C., Pertoft, H., and Smedsrød, B. (1983) Endothelial cells are a site of uptake and degradation of hyaluronic acid in the liver. *Exp. Cell Res.* **144,** 223–228
34. Fraser, J. R., Kimpton, W. G., Laurent, T. C., Cahill, R. N., and Vakakis, N. (1988) Uptake and degradation of hyaluronan in lymphatic tissue. *Biochem. J.* **256,** 153–158
35. Reed, R. K., Lilja, K., and Laurent, T. C. (1988) Hyaluronan in the rat with special reference to the skin. *Acta Physiol. Scand.* **134,** 405–411
36. Laurent, U. B., and Laurent, T. C. (1981) On the origin of hyaluronate in blood. *Biochem. Int.* **2,** 195–199
37. Camenisch, T. D., Spicer, A. P., Brehm-Gibson, T., Biesterfeldt, J., Augustine, M. L., Calabro, A., Jr., Kubalak, S., Klewer, S. E., and McDonald, J. A. (2000) Disruption of hyaluronan synthase-2 abrogates normal cardiac morphogenesis and hyaluronan-mediated transformation of epithelium to mesenchyme. *J. Clin. Invest.* **106,** 349–360
38. Węgrzyn, G., Jakóbkiewicz-Banecka, J., Narajczyk, M., Wiśniewski, A., Piotrowska, E., Gabig-Cimińska, M., Kloska, A., Słomińska-Wojewódzka, M., Korzon-Burakowska, A., and Węgrzyn, A. (2010) Why are behaviors of children suffering from various neuronopathic types of mucopolysaccharidoses different? *Med. Hypotheses* **75,** 605–609
39. Wood, K. M., Wusteman, F. S., and Curtis, C. G. (1973) The degradation of intravenously injected chondroitin 4-sulfate in the rat. *Biochem. J.* **134,** 1009–1013
40. Fischer, J. (1995) Tilorone-induced lysosomal storage of glycosaminoglycans in cultured corneal fibroblasts: biochemical and physicochemical investigations. *Biochem. J.* **312,** 215–222
41. Kawashima, H., Hirose, M., Hirose, J., Nagakubo, D., Plaas, A. H., and Miyasaka, M. (2000) Binding of a large chondroitin sulfate/dermatan sulfate proteoglycan, versican, to L-selectin, P-selectin, and CD44. *J. Biol. Chem.* **275,** 35448–35456
42. Harris, E. N., and Weigel, P. H. (2008) The ligand-binding profile of HARE: hyaluronan and chondroitin sulfates A, C, and D bind to overlapping sites distinct from the sites for heparin, acetylated low density lipoprotein, dermatan sulfate, and CS-E. *Glycobiology* **18,** 638–648
43. Aronson, N. N., Jr., and Davidson, E. A. (1967) Lysosomal hyaluronidase from rat liver. II. Properties. *J. Biol. Chem.* **242,** 441–444
44. Glaser, J. H., and Conrad, H. E. (1979) Chondroitin SO_4 catabolism in chick embryo chondrocytes. *J. Biol. Chem.* **254,** 2316–2325
45. Kaneiwa, T., Mizumoto, S., Sugahara, K., and Yamada, S. (2010) Identification of human hyaluronidase 4 as a novel chondroitin sulfate hydrolase that preferentially cleaves the galactosaminidic linkage in the trisulfated tetrasaccharide sequence. *Glycobiology* **20,** 300–309
46. Csóka, A. B., Scherer, S. W., and Stern, R. (1999) Expression analysis of six paralogous human hyaluronidase genes clustered on chromosomes 3p21 and 7q31. *Genomics* **60,** 356–361
47. Hardingham, T. E., and Muir, H. (1973) Binding of oligosaccharides of hyaluronic acid to proteoglycans. *Biochem. J.* **135,** 905–908
48. Hascall, V. C., and Heinegård, D. (1974) Aggregation of cartilage proteoglycans. II. Oligosaccharide competitors of the proteoglycan-hyaluronic acid interaction. *J. Biol. Chem.* **249,** 4242–4249